Turning without Fins: How Snakes Achieve High Maneuverability While Swimming

Elizabeth Gregorio, Ramiro Godoy-Diana, Anthony Herrel

Turning without Fins: How Snakes Achieve High Maneuverability While Swimming

Elizabeth Gregorio (1,2,*), Ramiro Godoy-Diana (1), and Anthony Herrel (2,3,4,5)
1 PMMH, CNRS, ESPCI Paris-PSL, Sorbonne Université, Université Paris Cité, Paris, France
2 UMR7179 MECADEV, Département Adaptation du Vivant, MNHN/CNRS, Paris, France
3 Department of Biology, Evolutionary Morphology of Vertebrates, Ghent University, K.L. Ledeganckstraat 35, Ghent 9000, Belgium
4 Department of Biology, University of Antwerp, Universiteitsplein 1, Wilrijk 2610, Belgium
5 Naturhistorisches Museum Bern, Bernastrasse 15, Bern 3005, Switzerland
* Correspondence: elizabeth.gregorio@espci.fr

Abstract (200 words)

The agile turning maneuvers of anguilliform swimmers remain one of the least studied aspects of aquatic locomotion, despite being crucial for survival in underwater environments. Turning is a difficult engineering problem because to change direction animals must minimize their moment of inertia while maximizing torque – two mathematical opposites. Anguilliform swimmers such as snakes are highly maneuverable and accomplish this goal without the aid of limbs or pectoral fins. In this study we explore how snakes manipulate their body position to change swimming direction by analyzing five turns by five individuals (four *Natrix maura* and one *Nerodia rhombifer*). We show that snakes curl their body inwards to shift their center of mass and reduce their moment of inertia when turning. We report a volumetric wake measurement for one turn which, together with the kinematics, allows us to quantify the timing between its change in moment of inertia and vortex shedding. Our results show that the snake only sheds vortices after it has minimized its moment of inertia. These results help explain how elongated anguilliform swimmers like snakes change swimming direction. They widen our understanding of how animals use transient maneuvers to navigate aquatic environments, with implications for both natural swimmers and underwater robots.

Introduction

When exploring aquatic environments animals engage in transitory swimming behaviors like turning and accelerating as often as forward swimming at constant speed. Some snakes even coil or tie their body to stabilize in the water column [1]. Yet, these common behaviors are under-represented in the literature. An exception are efforts to understand s- and c-start behaviors in fish [2-4]. Turning investigations are more recent, including wake measurements for turning jellyfish (*Aurelia aurita*) [5-6], squid (*Lolliguncula brevis*) [7], zebrafish (*Danio rerio*) [5,8], and giant danio (*Devario aequipinnatus*) [9]. Turning is a complex mechanical problem because it requires maximizing torque and minimizing moment of inertia – two mathematical opposites [5]. Species included in previous turning studies have been found to exploit their flexibility to manipulate the location of their propulsive surface (caudal fins and bell margin) to initiate the turn [5,6,8].

Anguilliform swimmers, like snakes, use their entire body to produce propulsion [10]. Their swimming mode, fin-less body, lack of propulsive jet, and length to diameter ratio separates them from the species whose turning mechanics have been previously studied. Snakes propagate a traveling wave along their body to crawl, swim, and fly [11-13]. Recent studies have shown that snakes, like other anguilliform swimmers, shed hairpin-shaped vortices at each bend along their body when swimming [14]. Their movement style and body shape enables their high maneuverability and eleven locomotor gaits [15]. These characteristics also likely require a different turning solution. Here, we combine wake measurements and moment of inertia estimates derived from kinematic observations to quantify how snakes change swimming direction.

Methods

To determine how snakes achieve high maneuverability in water we analyzed five trials in which the snake performed a voluntary turn. Our procedure and equipment is in accordance with Stin *et al.* 2023 with an added camera (acA3088-57uc, Basler) mounted above the tank all triggered at 14 Hz. Individuals performed this turn within the view of the kinematics camera and one individual performed its turn within view of both the kinematics camera and the 3D velocimetry system. We include two species: *Natrix maura* (4 individuals; #1, 2, 4, and 5) and *Nerodia rhombifer* (individual; # 3).

The snake's body was identified in each kinematics image recorded by the camera mounted above the tank to quantify each of the five unique turns. Superimposing these images illustrates the snake's high maneuverability through our range of turning observations (see Figure 1). We extract the center of mass from our kinematics images with the built in SciPy function. The center of mass is marked on each image in supplemental Figures S2 and S3. The moment of inertia is calculated as $I = m r^2$ where m is the body mass and r is the distance between the center of mass and the point along the body where the snake hinges or the head when swimming straight.

Individual #1 (6.1 g, 113 mm) turned inside the measurement volume (18 x 18 x 12 cm) of the volumetric three-component DDPTV setup (V3V-9000-CS system, TSI). This measurement allows us to quantify the velocity field around the snake as it turns. Our measurement includes velocity vectors on an evenly spaced vector grid (74 x 74 x 43) with a 2.5 mm resolution, 45 per body length (see Stin *et al.* 2023 for processing details). The Q-criterion of the vector field is computed to identify vortex structures where vorticity is greater than the viscous stress.

As the snake turns, its movements accelerate the fluid in the opposite direction of the snake's movement (see S1). Our wake measurements show the footprint of this momentum transfer. After identifying the generated vortices we apply Saffman's [16] definition of hydrodynamic impulse to quantify the momentum change required to instantaneously generate the vortex from a fluid at rest:

$$J = \frac{\rho}{2}\int_V x \times \omega \, dV$$

Where ρ is fluid density, V is vortex volume, x is the vector pointing from measurement volume's center to the center of V, and ω is the vorticity field. Newton's second law defines a force as the rate of change of momentum. This allows us to derive the vortex force by finding the quadratic line of best fit for the J of each vortex, taking the time derivative, and interpreting the slope as the fluid force reacting to the snake's movement through the fluid.

Results and Discussion

Although each snake follows a unique turning path, their moment of inertia profile follows the same pattern. Figure 1 shows that in each case the snake oscillates between relatively high and low moments of inertia. The local maxima and minima on the left of Figure 1 are circled and labeled to match the corresponding kinematics illustrated on the right. Typically, the snake appears to be in its usual swimming position when there is a maximum in the moment of inertia. There is one exception at (h) where the snake reaches a local maximum while in the midst of turning. This difference can be explained by comparing it to the global maximum for this individual which is much higher than the value observed at (h). This shows that the snake is still reducing its overall moment of inertia at (h).

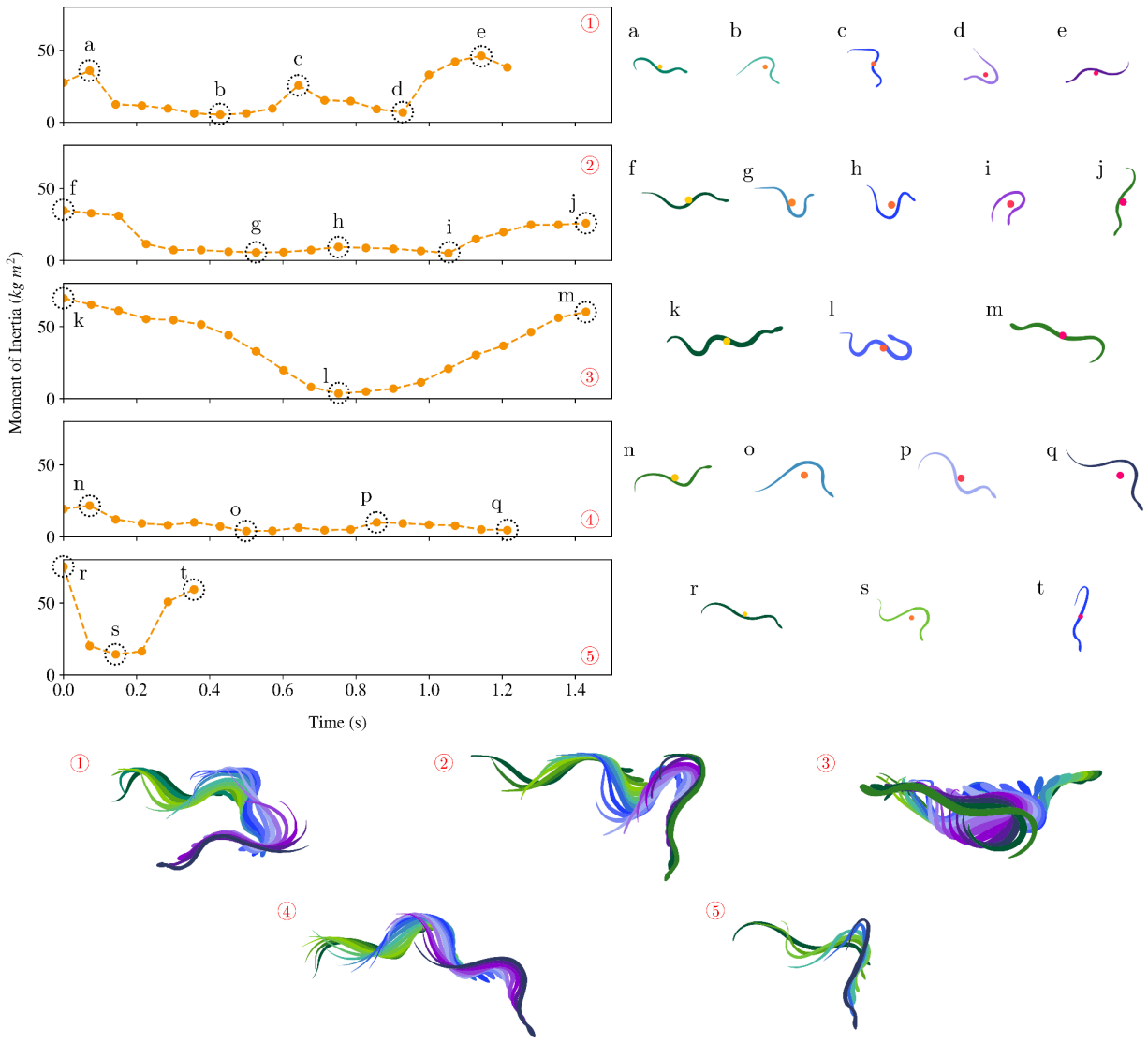

Figure 1: (left) Moment of inertia results for each turning snake with the local minima and maxima circled; (right) body position of each snake at the circled points with the center of mass marked with a circle. Colors on the left correspond to its layer in the superimposed kinematics of the full turn (bottom).

The shared method of turning between these snakes is perhaps best demonstrated by the body positions of the snakes when reaching a local minimum for their moment of inertia. At each example of this, shown at points b, d, g, i, l, o, q and s in Figure 1, the snake has curled its body inwards. Individuals #1, 2, 4, and 5 use the propagation of their traveling wave to bring their head and tail closer to the center of mass without interrupting their typical swimming pattern. Whereas individual #3 has interrupted its typical swimming pattern to pull its head and tail towards its center of mass at point l before unfolding to continue swimming in the opposite direction. These examples indicate that decreasing the moment of inertia is vital to turning behavior for swimming snakes and is similar to the decrease in moment of inertia seen for zebrafish and jellyfish by Dabiri *et. al.* (2020).

The volumetric wake measurements for individual #1 allows us to better understand the turning mechanism. This individual completed a u-shaped turn within the field of view of both the kinematics and wake measurement systems. The two measurement planes are perpendicular to each other – dorsal view for the kinematics and lateral view for the wake measurements. Figure 1 shows that #1 experiences two local minimums while turning, representing the two ninety degree turns that complete the u-shape.

The 3D wake measurements of this turn are shown in Figure 2 with the corresponding kinematics of this turn highlighted with a red box in S2. The first frame corresponds to point b in Figure 1 where the snake has pulled its body into a c-shape. Its tail flicks in the positive z direction generating a vortex that is visible in the first five frames of Figure 2 (1-1.29s). Then the snake turns its head in the negative x direction generating a vortex that is visible in frames 3-8 (1.14-1.5s). In frame 9 (1.57s), the body of the snake is curved like a hook and then the snake uncurls to complete the turn – generating a large vortex which is visible for the rest of the time series (1.57-1.79s).

When engaged in forward swimming, snakes and other anguilliform swimmers typically shed a vortex each time their body changes direction [14]. It is interesting that when turning we only see a vortex shedding event after large movements of the snake instead of at every curve along the snake's body. These not vortex shedding movements are undoubtedly building up vorticity along the body that our measurements cannot identify. However, we are able to identify them after they have been shed when the vorticity surpasses the shear stress. These results indicate that when turning the snake relies on movements to rearrange its body distribution that do not shed vortices.

The wake of a swimming animal is like a footprint that represents the transfer of momentum from the animal to the fluid (see S1). Therefore, by quantifying the wake we can reveal the turning mechanism. The hydrodynamic impulse is the momentum change required to instantaneously generate a given vortex from a state of rest. This value is calculated for the entire volume within the field of view at each time step. Hydrodynamic impulse is a vector and can therefore be broken into directional components to understand how the snake is moving within the three dimensional space. We report the full 4s swimming sequence recording, where J_x, J_y, and J_z are the hydrodynamic impulse along the three cartesian coordinates (see S2a). The kinematics (S2c) show that the snake swam roughly straight along the positive x axis from 0-1s and again along the negative x axis after completing its turn at 1.79s. The impulse plot does not show any deviation from 0 N/s until the turn begins because this portion of forward swimming is outside the measurement volume. The spike after the turning section around the 2s mark is due to the second portion of forward swimming. The wake measurements for this vortex are very similar to the results presented by Stin *et. al.* 2023 [14]. The snake then swims out of the field of view and the measured hydrodynamic impulse returns to 0 N/s.

The turning portion of the hydrodynamic impulse measurement is highlighted in red (S2b). Each of the three major vortex events are identifiable on this impulse plot. The first tail beat vortex (1-1.29s),

the vortex generated by the head turn (1.14-1.5s), and the large vortex generated by the snake flicking its tail as it comes out of the turn to resume straight swimming (1.57-1.79s). The third vortex represents the largest transfer of momentum from the snake to the fluid with the largest peaks being in positive x direction and negative y direction. In fact, 47% of the impulse is in the x direction, 46% in the y direction and 5% in the z direction at 1.57s when the vortex is at its largest size. After this peak, the vortex's impulse diminishes in size in the x and y directions while in the z direction the impulse increases before diminishing. The two tail beat vortices seem to appear directly after the minimum values in the snake's moment of inertia. The first vortex appears when the snake is at point b and the second tail beat vortex appears one time step after point d on Figure 1. This suggests that the snake sheds vortices after reaching a low moment of inertia when turning.

We can exploit the definition of force ($F = dJ/dt$) to calculate the vortex force for each of the shedding events. After identifying the vortices, we fit these data points with quadratic polynomials (S2b). The red curve for the first tail vortex, the orange for the second vortex generated by the head turn, and the green for the second tail beat vortex. These functions fit the data well and allow us to take the time derivative, using the slope as the vortex force (see Table 1).

Vortex Event	Time (s)	F_x	F_y	F_z
1	1.00-1.29	5.67e-04	-4.32e-03	-2.12e-03
2	1.14-1.50	-2.00e-03	2.54e-03	-7.41e-05
3	1.57-1.79	1.63e-02	-1.24e-03	-3.13e-02

Table 1: Vortex force (N) in each cardinal direction the three major vortex events: (1) first tail beat vortex, (2) vortex generated by head turn, (3) second tail beat vortex.

The vortex force calculated here is a representation of the reaction force generated by the snake as it turns in the water. In each case, the direction of the calculated vortex force is opposite to the movement of the snake at that moment. The snake generates the first vortex event by flicking its tail in the positive z direction to turn clockwise around the y axis. The vortex force is in the opposite direction, with the largest components in the negative z and y directions. The second vortex event is generated by the snake turning its head in the positive x direction so the vortex force is greatest in the negative x and positive y direction. The snake generates the third vortex event by uncurling its tail in the positive z direction so the vortex force is greatest in the negative z direction. There is vortex force in all three directions because fluid movement is always three dimensional and while most of the snake's movement is in the x-z plane there is some along the y axis. These vortex force measurements follow the results expected according to Newton's third law, in that they travel in the direction opposite to the snake's motion. Breaking the vortex force into the directional components provides more details about the direction of swimming and amount of propulsion required to complete the turn.

Conclusion

Our results demonstrate that snakes rearrange their body position and center of mass when turning to reduce their moment of inertia similarly to zebrafish and jellyfish [5]. We report the change in moment of inertia throughout five unique turns completed by five individual snakes. In each example they oscillate between relatively high and low moments of inertia to change direction. The wide range of turning behaviors demonstrates the diversity of ways that anguilliform swimmers with elongated bodies can change swimming direction.

Snakes use their entire body surface to accelerate fluid and produce propulsion when swimming. When engaged in forward swimming, a snake sheds a vortex at each bend along its body. We report volumetric wake measurements taken during the voluntary turn of individual #1 to show that when turning vortex shedding happens only after sudden movements. Our results indicate that snakes rely on body rearrangement movements to change the moment of inertia that do not result in vortex shedding. Once the snake has reached a minimum moment of inertia it generates a vortex to use the fluid's reactive force to complete the turn.

These results have uncovered a link between anguilliform swimmers' turning mechanism and the one employed by swimmers with an entirely different propulsion system. This interpretation of turning will be broadly applicable for elongated swimmers and bio-inspired robots. These experimental observations can also inform future computational fluid dynamics simulations of turning in anguilliform swimmers to fully compute the forces produced by the animal.

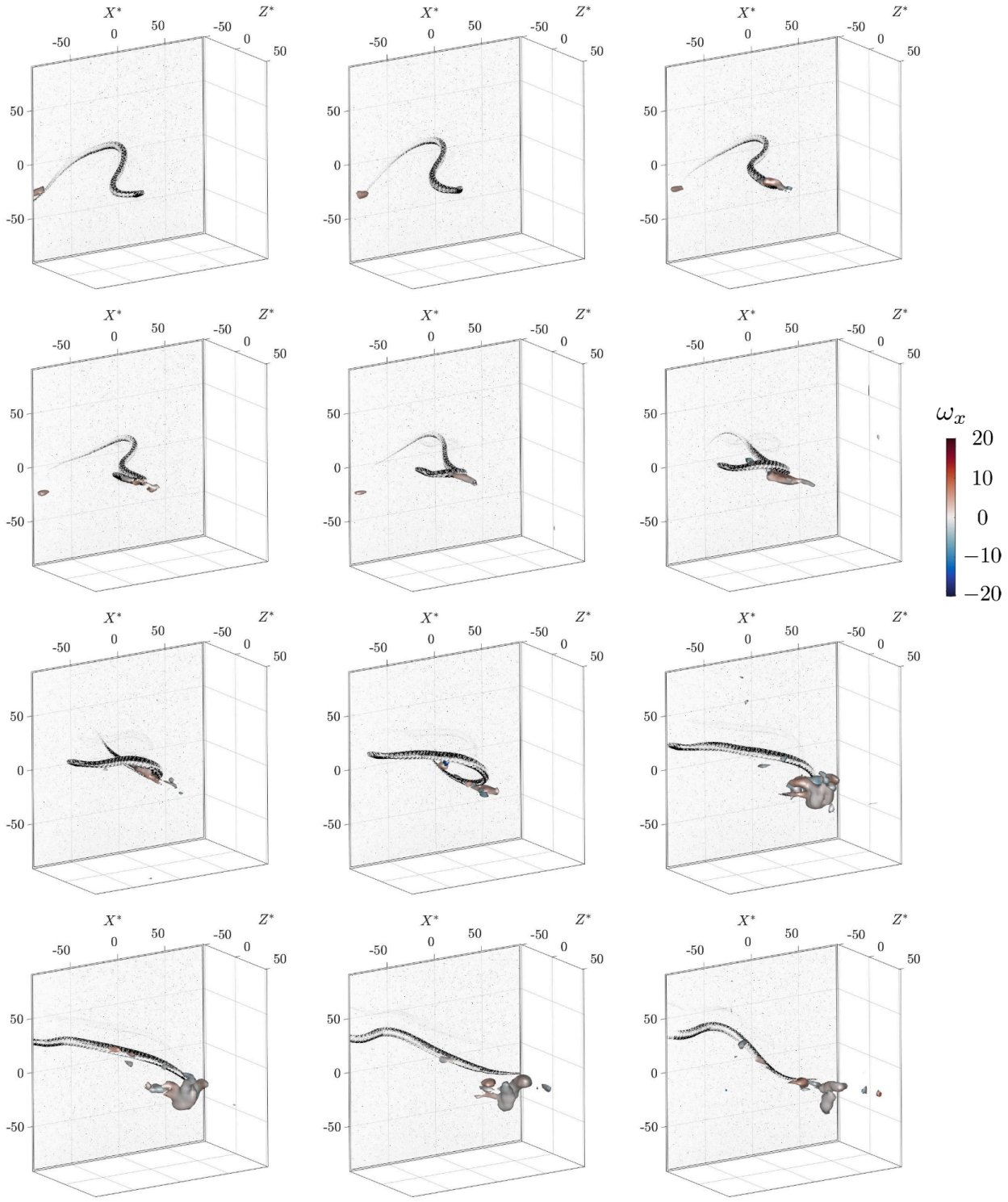

Figure 2: Time series of wake measurements taken while a *Natrix Maura* is turning, images begin with the 1s measurement and end with at 1.79s with 0.071s between images

References

1. Herault, J., Clement, É., Brossillon, J., LaGrange, S., Lebastard, V., and Boyer, F. (2020). Standing on the water: Stability mechanisms of snakes on free surface. Biomimetic and Biohybrid Systems: 9th International Conference, Living Machines 2020, Freiburg, Germany, July 28–30, 2020, Proceedings 9 (pp. 165-175). Springer International Publishing. 10.1007/978-3-030-64313-3_17
2. Domenici, P., and Blake, R.W. (1997). The kinematics and performance of fish fast-start swimming. Journal of Experimental Biology 200.8, 1165-1178. 10.1242/jeb.200.8.1165
3. Gazzola, M., Van Rees, W.M., and Koumoutsakos, P. (2012). C-start: optimal start of larval fish. Journal of Fluid Mechanics 698, 5-18. 10.1017/jfm.2011.558
4. Li, G., Müller, U.K., van Leeuwen, J.L., and Liu, H. (2014). Escape trajectories are deflected when fish larvae intercept their own C-start wake. Journal of The Royal Society Interface 11.101, 20140848. 10.1098/rsif.2014.0848
5. Dabiri, J.O., Colin, S.P., Gemmell, B.J., Lucas, K.N., Leftwich, M.C., and Costello, J.H. (2020). Jellyfish and fish solve the challenges of turning dynamics similarly to achieve high maneuverability. Fluids 5.3, 106. 10.3390/fluids5030106
6. Costello, J.H., Colin, S.P., Gemmell, B.J., Dabiri, J.O., and Kanso, E.A. (2024). Turning kinematics of the scyphomedusa Aurelia aurita. Bioinspiration & Biomimetics 19.2, 026005. 10.1088/1748-3190/ad1db8
7. Bartol, I.K., Ganley, A.M., Tumminelli, A.N., Krueger, P.S., and Thompson, J.T. (2022). Vectored jets power arms-first and tail-first turns differently in brief squid with assistance from fins and keeled arms. Journal of Experimental Biology 225.15, jeb244151. 10.1242/jeb.244151
8. Thandiackal, R., and Lauder, G.V. (2020) How zebrafish turn: analysis of pressure force dynamics and mechanical work. Journal of Experimental Biology 223.16, jeb223230. 10.1242/jeb.223230
9. Li, D.J., and Mendelson, L. (2023). Volumetric measurements of wake impulse and kinetic energy for evaluating swimming performance. Experiments in Fluids 64.3, 47. 10.1007/s00348-023-03586-y
10. Stin, V., Godoy‐Diana, R., Bonnet, X., and Herrel, A. (2024) Form and function of anguilliform swimming. Biological Reviews. 10.1111/brv.13116
11. Hu, D.L., Nirody, J., Scott, T., and Shelley, M.J. (2009). The mechanics of slithering locomotion. Proceedings of the National Academy of Sciences 106.25, 10081-10085. 10.1073/pnas.0812533106
12. Jayne, B.C. (1985). Swimming in constricting (Elaphe g. guttata) and nonconstricting (Nerodia fasciata pictiventris) colubrid snakes. Copeia, 195-208. 10.2307/1444809
13. Socha, J.J., O'Dempsey, T., and LaBarbera, M. (2005) A 3-D kinematic analysis of gliding in a flying snake, Chrysopelea paradisi. Journal of Experimental Biology 208.10, 1817-1833. 10.1242/jeb.01579
14. Stin, V., Godoy‐Diana, R., Bonnet, X., and Herrel, A. (2023) Measuring the 3D wake of swimming snakes (Natrix tessellata) using volumetric particle image velocimetry. Journal of Experimental Biology 226.13, jeb245929. 10.1242/jeb.245929
15. Jayne, B.C. (2020) What defines different modes of snake locomotion?. Integrative and comparative biology 60.1, 156-170. 10.1093/icb/icaa017
16. Saffman, P.G. (1995). Vortex dynamics (Cambridge university press).

Data Availability

- All data and code required to produce the Figures and Tables included in this report and supplementary material are included in the repository. Authors are available for questions or to provide additional material.

Acknowledgements

We would like to acknowledge the interns that aided E.G. with data collection: Olivia Alves, Lauréanne Feral, and Johannes Marchand.

Author Contributions

- E.G., A.H. and R.G.D. conceived the study; E.G. carried out experimental work; E.G. carried out data analysis; E.G. wrote the manuscript; E.G., A.H. and R.G.D. revised the manuscript. All authors gave final approval for publication.

Funding

- This work is funded by the Agence Nationale de la Recherche (France) through project DRAGON2 (ANR-20- CE02-0010).

Competing interests

- Authors have no competing interests to disclose

Supplementary Material

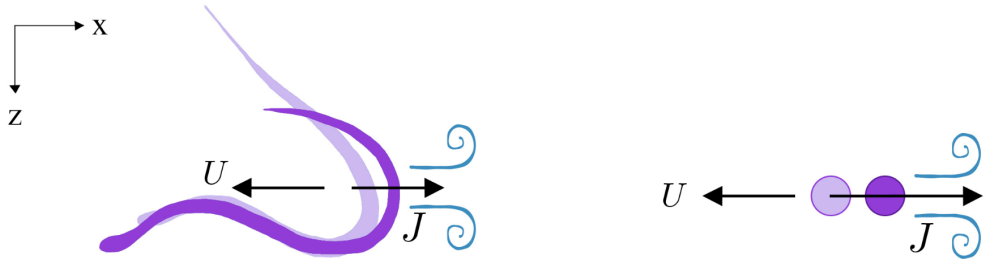

SM Figure 1: Sketch of snake traveling at velocity U by flicking its tail to generate impulse (J).

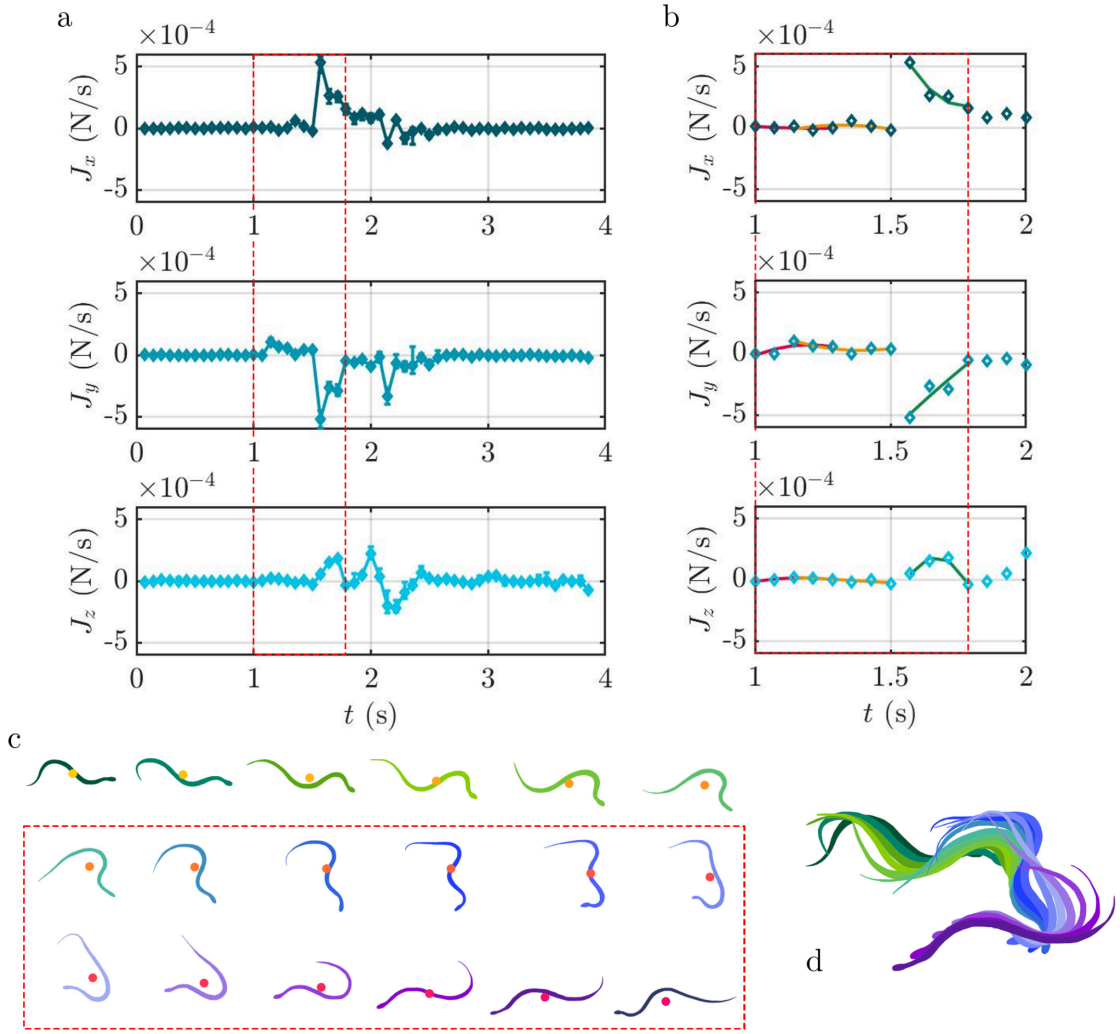

SM Figure 2: Quantification of the turn highlighted by red boxes for the (a) hydrodynamic impulse throughout the recording (error bars reflect increase or decrease of Q-criterion by 1) and (b) during the turn with quadratic best fit for each vortex event, and swimming kinematics (c) with center of mass marked. (d) Shows all kinematic images superimposed.

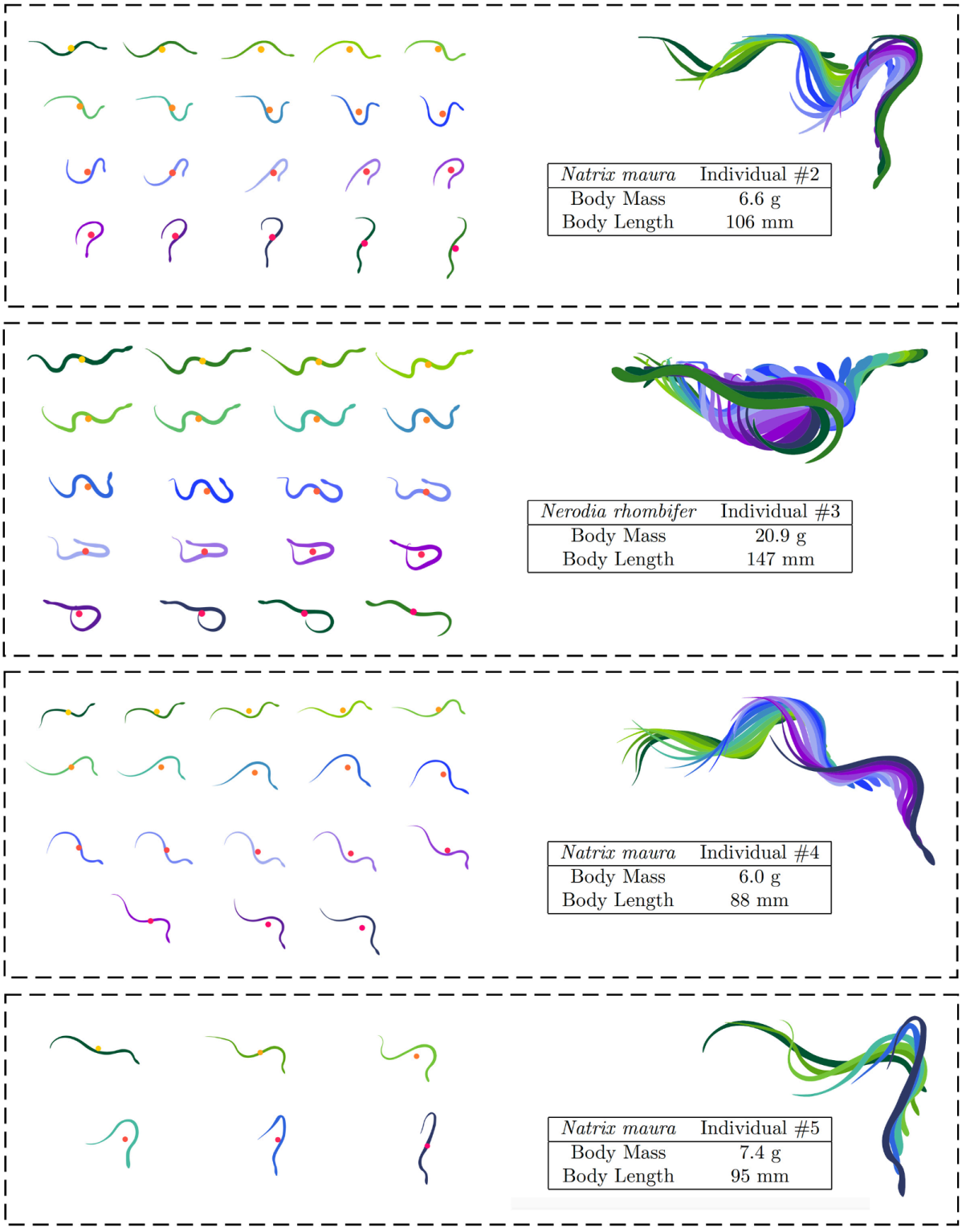

SM Figure 3: Kinematics of observed turns for three additional *Natrix maura* individuals (2,4,5) and one *Nerodia rhombifer* individual (3): left panel shows the center of mass location while turning, superimposed kinematics, and body size measurements.